Published in final edited form as:
Toxicol Appl Pharmacol. 2014 May 1; 276(3): 179–187. doi:10.1016/j.taap.2014.02.011.

Acute 7,12-dimethylbenz[a]anthracene exposure causes differential concentration-dependent follicle depletion and gene expression in neonatal rat ovaries

Jill A. Madden[1], **Patricia B. Hoyer**[2], **Patrick J. Devine**[3,4], and **Aileen F. Keating**[1,2,†]

[1]Department of Animal Science, Iowa State University, Ames, IA 50011

[2]Department of Physiology, University of Arizona, Tucson, AZ 85724

[3]INRS–Institut Armand-Frappier Research Centre, University of Quebec, Laval, QC H7V 1B7, Canada

Abstract

Chronic exposure to the polycyclic aromatic hydrocarbon 7,12-dimethylbenz[a]anthracene (DMBA), generated during combustion of organic matter including cigarette smoke, depletes all ovarian follicle types in the mouse and rat, and *in vitro* models mimic this effect. To investigate the mechanisms involved in follicular depletion during acute DMBA exposure, two concentrations of DMBA at which follicle depletion has (75 nM) and has not (12.5 nM) been observed were investigated. Postnatal day four F344 rat ovaries were maintained in culture for four days before a single exposure to vehicle control (1% DMSO; CT) or DMBA (12 nM; low-concentration or 75 nM; high-concentration). After four or eight additional days of culture, DMBA-induced follicle depletion was evaluated via follicle enumeration. Relative to control, DMBA did not affect follicle numbers after 4 days of exposure, but induced large primary follicle loss at both concentrations after 8 days; while, the low-concentration DMBA also caused secondary follicle depletion. Neither concentration affected primordial or small primary follicle number. RNA was isolated and quantitative RT-PCR performed prior to follicle loss to measure mRNA levels of genes involved in xenobiotic metabolism (*Cyp2e1*, *Gstmu*, *Gstpi*, *Ephx1*), autophagy (*Atg7*, *Becn1*), oxidative stress response (*Sod1*, *Sod2*) and the phosphatidylinositol 3-kinase (PI3K) pathway (*Kitlg*, *cKit*, *Akt1*) 1, 2 and 4 days after exposure. With the exception of *Atg7* and *cKit*, DMBA increased ($P < 0.05$) expression of all genes investigated. Also, BECN1 and pAKT^{Thr308} protein levels were increased while cKIT was decreased by DMBA exposure. Taken together, these results suggest an increase in DMBA bioactivation, add to the mechanistic understanding of DMBA-induced ovotoxicity and raise concern regarding female low concentration DMBA exposures.

[†]**Corresponding author:** Aileen F. Keating, Ph.D., Department of Animal Science, Iowa State University, Ames, IA 50011. akeating@iastate.edu; Telephone number: 1-515-294-3849; Fax number: 1-515-294-4471.
[4]Current address: Novartis Institutes for Biomedical Research Inc, Cambridge, MA 02139, USA

Keywords

DMBA; ovary; follicle

Introduction

The ovary contains a finite number of oocyte-containing follicles. Appropriate maturation and survival through the primordial, small primary, large primary, secondary, and antral follicular stages is essential for both conception and female health. The primordial is most immature follicular stage, in which the oocyte remains arrested in meiosis and waits for an appropriate signal to enter into the growing follicular pool toward ovulation. Once the ovarian primordial follicular reserve is depleted, ovarian failure occurs, rendering the female both infertile and at an increased risk for development of a variety of health conditions including osteoporosis and heart disease (Greendale *et al.*, 1999).

Follicles are vulnerable to toxic exposures at all developmental stages. 7,12-dimethylbenz[a]anthracene (DMBA), a polycyclic aromatic hydrocarbon (PAH), is produced from the burning of organic material (Gelboin, 1980), thus cigarette smoke is an exposure source. DMBA depletes all ovarian follicle types in mice and rats (Mattison and Schulman, 1980) and is the most ovotoxic of three PAH cigarette smoke-components (DMBA, 3-methylcholanthrene and benzo[a]pyrene (Borman *et al.*, 2000). An acute high-concentration exposure to DMBA *in vivo* destroyed primordial oocytes in rats and mice (Mattison, 1979; Mattison and Thorgeirsson, 1979), and use of an ovary culture system has demonstrated that repeated exposures of DMBA to F344 rat ovaries caused primordial follicle loss at concentrations of 75 nM and higher (Igawa *et al.*, 2009). In support of the ovotoxicity of DMBA (and other cigarette smoke components), ovarian failure onset is accelerated in female cigarette smokers (Jick and Porter, 1977).

In order for ovotoxicity to ensue, DMBA must be bioactivated to an ovotoxic metabolite; DMBA-3,4-diol, 1,2-epoxide (Miyata *et al.*, 1999; Igawa *et al.*, 2009), by a number of enzymes including microsomal epoxide hydrolase (*Ephx1*). Using the *in vitro* postnatal day (PND) 4 ovarian culture system, competitive inhibition of EPHX1 by cyclohexene oxide reduced DMBA-induced follicle loss in ovaries from mice (1 μM DMBA; Rajapaksa *et al.*, 2007) and rats (1 μM DMBA; Igawa et al., 2009). Furthermore, mRNA levels of *Ephx1* increased after 2 days of DMBA exposure, prior to follicle loss which occurs after 4 days, relative to control (Rajapaksa *et al.*, 2007; Igawa *et al.*, 2009). Additionally, cytochrome P450 isoform 2E1 (*Cyp2e1*)-null mice had increased sensitivity to DMBA-induced primordial and small primary follicle loss (Keating *et al.*, 2008). This was at least in part due to increased *Ephx1* levels in the *Cyp2e1*-null ovaries. Thus, the action of ovarian EPHX1 is critical for DMBA to impart its ovotoxicant effects, and *Cyp2e1* and *Ephx1* regulation are in some way interrelated (Keating *et al.*, 2008).

Previous studies have suggested that the phosphatidylinositol 3-kinase (PI3K) pathway plays a role in *Ephx1* expression regulation (Kim *et al.*, 2003; Bhattacharya *et al.*, 2012). Specifically, PI3K inhibition using LY294002 in cultured F344 rat ovaries resulted in increased *Ephx1* mRNA and protein expression (Bhattacharya *et al.*, 2012), while decreased

EPHX1 was observed following PI3K inhibition in rat hepatocytes (Kim *et al.*, 2003). Despite these tissue-specific responses, a link between *Ephx1* gene expression and the PI3K pathway is supported.

In addition to its role in xenobiotic biotransformation via *Ephx1* regulation, the PI3K pathway is vital for follicle survival and recruitment, particularly pre-antral follicles (Yoshida *et al.*, 1997; Parrott and Skinner, 1999; Castrillon *et al.*, 2003; Keating *et al.*, 2009). Initiation of the PI3K signaling pathway occurs once the granulosa-derived signaling molecule Kit ligand (KITLG) binds the oocyte-expressed stem cell receptor (cKIT; Ismail *et al.*, 1996). Following KITLG-cKIT interaction, the PI3K signaling cascade is activated leading to phosphorylation of the downstream effector molecule protein kinase B (AKT) and subsequently the forkhead transcription factor 3a (FOXO3a), both important for control of primordial follicle survival and recruitment, respectively (Castrillon *et al.*, 2003; Reddy *et al.*, 2005; Liu *et al.*, 2006; John *et al.*, 2008). *Foxo3a*-null mice suffer from follicular depletion and ovarian failure as a result of global follicle activation (Castrillon *et al.*, 2003), while oocyte-specific FOXO3a overexpression restricts primordial follicles from entering the recruitment pool, also rendering the female infertile (Liu *et al.*, 2006).

The ovarian response to oxidative stress is also important for follicle viability. Reactive oxygen species (ROS) have been shown to increase prior to DMBA-induced follicle loss *in vitro*, suggesting that DMBA exposure (0.1–100 μM) induces oxidative stress within the ovary (Tsai-Turton *et al.*, 2007). Co-treatment with DMBA (10 μM) and glutathione (GSH; which detoxifies ROS) alleviated DMBA-induced follicle loss (Tsai-Turton *et al.*, 2007), further supporting that DMBA induces ROS generation. Reactive xenobiotics can also be detoxified through GSH conjugation catalyzed by the glutathione *S*-transferase (GST) family of enzymes (Reddy *et al.*, 1983). GST isoform pi (*Gstp*) mRNA and protein increase following DMBA exposure in the cultured neonatal F344 rat ovary prior to the onset of follicle loss (Bhattacharya and Keating, 2012). Furthermore, mice that are deficient in GSTPI have increased levels of DMBA-induced skin tumors (Henderson *et al.*, 1998), indicating that GSTP-catalyzed GSH conjugation to DMBA is a potential detoxification event.

In addition to ROS alleviation by GSH, superoxide dismutases (SOD1 – cytoplasmic; SOD2 - mitochondrial) can act directly on superoxide anion radicals to form water and hydrogen peroxide. Studies have shown that *Sod1*-null mice exhibit reduced fertility (Ho *et al.*, 1998; Matzuk *et al.*, 1998), while although *Sod2*-deficient mice die pre-pubertally, when SOD-deficient ovaries are transplanted to wild-type mice, reproductive abnormalities are not observed (Matzuk *et al.*, 1998).

As an alternative to apoptosis (Morita and Tilly, 1999; Hu *et al.*, 2001), another form of programmed cell death, autophagy, may contribute to follicle depletion. When activated, autophagy induces the formation of an autophagosome, which, once fused with the lysosome, can consume internal components of a cell (Levine and Klionsky, 2004). Several proteins are involved in the process of autophagy including Autophagy-related protein 7 (ATG7) and Beclin-1 (BECN1; Kim *et al.*, 1999; Liang *et al.*, 1999). ATG7 and BECN1 are of particular interest in the ovary due to previous evidence suggesting their involvement in

autophagy for female germ cell survival (Gawriluk *et al.*, 2011). Further evidence supporting involvement of autophagy during DMBA-induced ovotoxicity has come from work demonstrating that cigarette smoke exposure (a source of DMBA) induced autophagy in the ovaries of exposed mice (Gannon *et al*., 2012; 2013). Thus autophagy could potentially be involved during DMBA-induced follicle loss.

It is difficult to estimate human DMBA ovarian exposure due to differences in hepatic bioactivation between individuals. For this reason, the ovotoxic effects of repeated DMBA exposures have been investigated using the PND4 *in vitro* ovary culture system at a concentration (1 μM) that causes approximately 50% primordial follicle loss after 4 days (Rajapaksa *et al*., 2007; Igawa *et al*., 2009). Additionally, these exposures have been previously administered from the onset of culture when the ovary is largely comprised of primordial follicles. The current study was designed to delay exposure to DMBA until after 4 days of culture in order to determine the impact of DMBA exposure on large primary and secondary follicles. Also, single DMBA exposures were used to determine the impact of low concentration acute exposures to DMBA, similar to that of passive cigarette smoke exposure, on ovarian function. The ovarian response to acute DMBA exposure was examined by quantifying follicle numbers and measuring the mRNA levels of genes involved in 1) xenobiotic biotransformation - *Cyp2e1*, *Ephx1*, *Gstpi* and *Gstmu*; 2) PI3K signaling - *Akt1*, *cKit* and *Kitlg*; 3) the oxidative stress response - *Sod1* and *Sod2*; and 4) autophagy - *Atg7* and *Becn1*. Also, levels of EPHX1, BECN1, cKIT and pAKT^{Thr308} in ovaries treated with control, low (12.5 nM) or high (75 nM) DMBA were evaluated.

Materials and Methods

Reagents

7,12-dimethylbenz[a]anthracene (DMBA), bovine serum albumin (BSA), ascorbic acid, transferrin, 2-β-mercaptoethanol, 30% acrylamide/0.8% bisacrylamide, ammonium persulphate, glycerol, N' N' N' N'-Tetrathylethylenediamine (TEMED), Tris base, Tris HCL, sodium chloride, Tween-20 were purchased from Sigma Aldrich Inc. (St. Louis, MO). Dulbecco's Modified Eagle Medium: nutrient mixture F-12 (Ham) 1x (DMEM/Ham's F12), Albumax, penicillin (5000U/ml) Hank's Balanced Salt Solution (without $CaCl_2$, $MgCl_2$, or $MgSO_4$) were obtained from Invitrogen Co. (Grand Island, NY). Millicell-CM filter inserts and 48-well cell culture plates were obtained from Millipore (Billerica, MA) and Corning Inc. (Corning, NY), respectively. RNeasy Mini kit, QIA Shredder kit, RNeasy Mini Elute kit, and Quantitect™ SYBR Green PCR kit were purchased from Qiagen Inc. (Valencia, CA). RNA*later* was obtained from Ambion Inc. (Grand Island, NY). With the exception of *cKit* and *Kitlg* which were obtained from Integrated DNA Technologies (Coralville, IA), all primers were obtained from the DNA facility of the Iowa State University office of biotechnology (Ames, IA). Anti-EPHX1 antibody was from Detroit R&D (Detroit, MI). Anti-pAKT^{Thr308} was purchased from Abcam Technology (Cambridge, MA) and Cell Signaling Technology (Danvers, MA). Anti-BECN1 and anti-cKIT were obtained from Santa Cruz (Dallas, TX) and Cell Signaling Technology (Danvers, MA), respectively.

Animals

Fisher 344 (F344) rats (approximately 6 months of age) were housed in plastic cages and maintained in a controlled environment (22 ± 2°C; 12h light/12h dark cycles). The animals were provided a standard diet with *ad libitum* access to food and water, and housed with a proven male for 5 days (two females per male). Approximately 2–3 days before parturition date, females were separated and housed one per cage and allowed to give birth. The University of Arizona and Iowa State University Institutional Animal Care and Use Committee's approved all experimental procedures.

In vitro ovarian cultures

Ovaries were collected from female PND4 F344 rats and cultured as described by Devine *et al.*, 2002. The PND4 rat pups were euthanized by CO_2 inhalation followed by decapitation. Ovaries were removed, trimmed of oviduct and other excess tissue, and placed onto a Millicell-CM membrane floating on 250 μl of previously 37°C equilibrated DMEM/Ham's F12 medium containing 1 mg/ml BSA, 1 mg/ml Albumax, 50 μg/ml ascorbic acid, 5 U/ml penicillin and 27.5 μg/ml transferrin per well in a 48-well plate. A drop of medium was placed on top of each ovary to prevent dehydration. Ovaries were cultured at 37°C and 5% CO_2 for 4 days, then treated with vehicle control media (1% DMSO), low DMBA (12.5 nM) or high DMBA (75 nM) for an additional 1, 2, 4 or 8 days. This time of exposure ensured that large primary and secondary ovarian follicles were present at time of treatment.

Histological evaluation of follicle numbers

Following 4 or 8 days of culture, ovaries were placed in 4% paraformaldehyde for 2 hours, washed and stored in 70% ethanol, paraffin embedded, and serially sectioned (5 μM). Every 6^{th} section was mounted and stained with hematoxylin and eosin. Healthy oocyte-containing follicles were identified and counted in every 6^{th} section. Follicles were considered primordial if they contained an oocyte surrounded with a single layer of squamous-shaped granulosa cells; small primary if they contained an oocyte surrounded by ≤ 10 cuboidal-shaped granulosa cells; large primary if they contained an oocyte surrounded by > 10 cuboidal shaped-granulosa cells; and secondary if they contained an oocyte surrounded by multiple layers of granulosa cells. Unhealthy/atretic follicles were distinguished from healthy follicles by the appearance of pyknotic bodies and intense eosinophilic staining of oocytes. Healthy follicles were classified and enumerated according to Flaws *et al.*, 1994. Slides were blinded to prevent counting bias.

RNA isolation and polymerase chain reaction (PCR)

Following 1, 2 or 4 days post-treatment, ovaries were stored in RNA*later* at −80°C. Total RNA was isolated from ovaries (n=3; 6 ovaries per pool) using an RNeasy Mini kit according to the manufacturer's instructions. RNA was eluted in 14 μl of RNase-free water and concentration quantified using a NanoDrop (λ = 260/280 nm; ND 1000; Nanodrop Technologies Inc., Wilmington, DE). Total RNA (150 ng) was reverse transcribed to cDNA using the Superscript III One-Step RT-PCR System. Genes of interest were amplified using an Eppendorf mastercycler (Hauppauge, NY) using a Quantitect ™ SYBR Green PCR kit (Qiagen Inc. Valencia, CA). The primers used are listed in Table 1. The PCR conditions

used were a 15 min hold at 95°C and 40 cycles of denaturing at 95°C for 15 s, annealing at 58 °C for 15 s, and extension at 72°C for 20 s. Changes in gene expression were quantified using the $2^{-\Delta\Delta Ct}$ method (Livak and Schmittgen, 2001; Pfaffl, 2001). It should be noted that DMBA exposure impacted expression of a number of housekeeping genes (β-actin, cyclophilin B, and hypoxanthine phosphoribosyltransferase 1, data not shown), with the exception of *Gapdh* and 18S rRNA. *Gapdh* was chosen as the housekeeping gene.

Immunofluorescence staining

Following treatment, ovaries were placed in 4% paraformaldehyde for 2 hours, washed and stored in 70% ethanol, paraffin embedded and serially sectioned (5 μM). Two sections per ovary (n = 3) were deparaffinized and incubated with primary antibodies (1:50 dilution) directed against EPHX1, $pAKT^{Thr308}$, BECN1 or cKIT at 4°C overnight. The blocking solution used was 5% BSA. Secondary FITC antibody was applied for 1 h, followed by Hoechst (30 minutes; 5mg/ml). Slides were repeatedly rinsed with PBS, cover-slipped, and stored in the dark (4°C) until visualization. Primary antibody was not added to immunonegative ovarian sections. Immunofluorescence was visualized on a Leica DMI300B fluorescent microscope at λ = 488 and 633 nm for FITC and Hoechst, respectively. All images were captured using a 10× objective lens. Protein staining was quantified using ImageJ software by circling the follicle under analysis and measuring integrated density. An identical measurement area was maintained between follicles of a particular stage. Integrated density of EPHX1, pAKT, and cKIT protein staining was measured in ten small (primordial and small primary) follicles and five large (large primary and secondary) follicles per section. The average number of follicles analyzed per ovary was 20 small and 10 large. BECN1 protein abundance was evaluated via quantification of the total number of foci present in each section. Statistical analysis was performed by comparison between control and treatment on day of staining. When statistical difference was observed for all three staining repetitions, an effect of treatment on the protein of interest was concluded. For ease of presentation, control treatment is presented as 100% and the DMBA treatments are expressed as a percentage of control. Statistical difference is from the raw data.

Statistical analysis

Comparisons were made between treatments for follicle count experiments using Analysis of Variance (ANOVA). Quantitative RT-PCR and immunofluorescence staining data were analyzed by t-test comparing treatment with control raw data at each individual time-point. All statistical analyses were performed using Prism 5.04 software (GraphPad Software). Statistical significance was defined as $P < 0.05$.

Results

Effect of acute DMBA exposure on ovarian histology and follicle number

To investigate the effects of acute low and high DMBA exposures on follicle viability and ovarian morphology, PND4 ovaries were exposed once after 4 days of culture and the ovaries were maintained for an additional 4 (Figure 1A – D) or 8 (Figure 2A – H) days. There was no impact of a single exposure to DMBA at either concentration on primordial,

small primary or large primary follicles after 4 days in culture. Interestingly, there were increased ($P < 0.05$) secondary follicle number at the low DMBA concentration. Additionally, DMBA did not induce primordial or small primary follicle loss at either concentration 8d after exposure (Figure 2A-1F). Both DMBA concentrations induced large primary follicle loss ($P < 0.05$; Figure 2G). Interestingly, only the low DMBA concentration induced secondary follicle loss ($P < 0.05$; Figure 2H).

In addition to follicle depletion, DMBA single exposure caused morphological alterations in both large primary and secondary follicles. Shrunken, eosinophilic oocytes resulting from an apparent loss of connection between the oocyte and granulosa cells occurred at both concentrations. Intense eosinophilic staining of follicles also indicated significantly more atretic follicles in ovaries exposed to DMBA (Figure 2D).

Effect of acute DMBA exposures on mRNA expression

Temporal pattern of single DMBA exposure on expression of genes involved in chemical metabolism—*Cyp2e1* mRNA was increased ($P < 0.05$) by both DMBA treatments after 4d of exposure, and there was a trend ($P < 0.1$) for an increase after 2d. Interestingly, the low DMBA exposure induced a greater increased in *Cyp2e1* at the 4d timepoint (Figure 3A). *Gstpi* was increased ($P < 0.05$) in a temporal and concentration dependent pattern by the high and low DMBA exposures increasing *Gstpi* mRNA level after 1d and 4d, respectively (Figure 3B). There was no impact of DMBA exposure on *Gstmu* mRNA until 4d in the low exposure when *Gstmu* was increased ($P < 0.05$; Figure 3C). *Ephx1* mRNA was increased ($P < 0.05$) by low DMBA after 4d, with a trend ($P < 0.1$) for a lesser increase at the high DMBA concentration after 2d of exposure (Figure 3D).

Induction of genes involved in oxidative stress response by DMBA exposure—Both DMBA exposures increased ($P < 0.05$) *Sod1* mRNA after 2d, however, this increase was returned to control levels after 4d in the high DMBA exposure, while there was a trend ($P < 0.1$) for increased *Sod1* to be maintained after 4d at the low DMBA exposure (Figure 4A). *Sod2* was increased at the high DMBA exposure after 2d, and there was a trend for an increase in *Sod2* by the low DMBA ($P = 0.1$) after 2d (Figure 4B).

Induction of autophagy genes by single DMBA exposure—There was no impact of high DMBA exposure on *Atg7* mRNA expression, however, the low concentration tended ($P < 0.1$) to reduce *Atg7* mRNA after 2d with a further decrease ($P < 0.05$) after 4d (Figure 5A). *Becn1* mRNA was increased by low DMBA after 2d ($P < 0.1$) and 4d ($P < 0.05$) while high DMBA tended to increase *Becn1* after 2d with a return to basal levels after 4d (Figure 5B).

Impact of DMBA exposure on PI3K gene expression—There was a temporal concentration dependent pattern of *Kitlg* induction with the high DMBA exposure increasing *Kitlg* after 2d, while the low DMBA exposure lagged and induced *Kitlg* mRNA after 4d. There was also a trend for induced *Kitlg* after 2d in the low DMBA exposure (Figure 6A). Neither concentration of DMBA affected *cKit* mRNA level (Figure 6B), while there was also a temporal concentration dependent pattern of *Akt1* mRNA induction (Figure 6C). The

high DMBA exposure induced increased ($P < 0.05$) *Akt1* mRNA after 1d, was at control levels after 2d but increased ($P < 0.05$) again after 4d of exposure. At the low DMBA concentration, *Akt1* was increased ($P < 0.05$) after 2 and 4d of exposure (Figure 6C).

Effect of acute DMBA exposure on protein localization and level

EPHX1 protein was localized to the oocyte cytoplasm and interstitial tissue. No impact of DMBA exposure on EPHX1 protein was observed in the oocyte cytoplasm or in the ovary as a whole at either DMBA concentration (Figure 7A–D). BECN1 protein appeared as punctate foci localized mainly in the granulosa cell layer. A greater number of BECN positive foci were observed in ovaries treated with 12.5 nM DMBA, relative to control or 75 nM DMBA treated ovaries (Figure 7E–H). cKIT was localized to the oocyte cytoplasmic membrane of primordial and small primary follicles. There was a trend for decreased cKIT protein concentration in 75 nM DMBA treated ovaries but no impact of 12.5 nM DMBA related to control treated ovaries (Figure 7I–L). Finally, $pAKT^{Thr308}$ was present in the oocyte cytoplasm of follicles of all stages. Quantification of $pAKT^{Thr308}$ demonstrated higher levels ($P < 0.05$) in the oocytes of small and large follicles exposed to 12.5 nM DMBA relative to control and in the large follicles in 75 nM DMBA-treated ovaries (Figure 7M–P).

Discussion

DMBA is an ovotoxicant that causes follicle depletion, ultimately resulting in ovarian failure (Keating *et al*., 2008; Igawa *et al*., 2009; Nteeba et al., 2014). This study was designed to focus on effects of DMBA on large primary and secondary follicles by allowing these follicles to develop in culture before DMBA exposure. Previously, follicle loss was observed after continuous exposure (alternate days) to 75 nM DMBA but not 12.5 nM (Igawa *et al*., 2009). Relative to control, we observed that a single concentration of DMBA at either concentration did not deplete primordial or small primary follicles at either timepoint examined, while both DMBA concentrations depleted large primary follicles. The low DMBA concentration caused loss of secondary follicles also. These data support that even low level acute DMBA exposures can affect and deplete the number of large primary and secondary follicles, potentially causing temporary infertility in exposed females. While previous studies have shown that all stage follicles are depleted by DMBA (Rajapaksa *et al*., 2007; Igawa *et al*., 2009), our data may suggest that the larger follicles could be the initial targets of DMBA, and that depletion of smaller follicles stages may be a consequence of loss of larger follicles, that is, increased recruitment from the pool of smaller follicles may occur to replace the larger follicles that have been lost. Alternatively, it may be that higher DMBA concentrations can directly deplete the primordial and small primary follicle pools, as has been observed previously (Igawa *et al*., 2009). Taken together, these data support that acute, low-level DMBA exposure represents a valid female health concern and warrants attention.

It was both interesting and surprising that there appeared to be a difference in depletion of the large primary and secondary follicles between low and high DMBA exposures, which led to the hypothesis that DMBA may induce concentration-dependent differential ovarian gene expression in the neonatal rat ovary. Over a timecourse of DMBA exposure we

discovered that both concentrations increased *Cyp2e1* mRNA level, and this was highest at the low DMBA concentration. Though there is little data in the literature to suggest that CYP 2E1 is involved in DMBA biotransformation, our data showing that ovarian *Cyp2e1* mRNA level increases in response to DMBA exposure suggests that this gene is responsive to DMBA exposure and may support a role for CYP2E1 in DMBA metabolism. In support of this possibility, *Cyp2e1*-null mice exposed to DMBA (0.5μM and higher) exhibited greater primordial and small primary follicle loss relative to controls (Keating *et al.*, 2008).

The GST family of enzymes mediate xenobiotic metabolism by conjugating GSH to compounds, promoting excretion from the body (Reddy *et al.*, 1983). In cultured rat pre-ovulatory follicles, co-treatment with GSH during DMBA exposure lessened follicle apoptosis (Tsai-Turton *et al.*, 2007) suggesting the possible involvement of GST enzymes in catalyzing detoxification of DMBA. *Gstpi* has previously been identified to be involved in the ovarian response to DMBA exposure in neonatal rat ovaries (Bhattacharya and Keating, 2012), and adult mice exposed to DMBA (Nteeba *et al*., 2014). *Gstpi*-null mice are also more sensitive to DMBA-induced skin tumors (Henderson *et al*., 1998). GSTMU has also been demonstrated to be increased in response to DMBA in the ovaries from obese adult mice (Nteeba *et al*., 2014). In addition to the role of GSTPI and GSTMU in catalyzing GSH conjugation to xenobiotics, they can also play a role in inhibiting the pro-apoptotic proteins c-Jun N-terminal Kinase (JNK) (Keating *et al.*, 2010; Bhattacharya and Keating, 2012) and apoptosis signal-regulating kinase 1 (ASK1) (Bhattacharya *et al.*, 2013). The current study determined that *Gstmu* is increased by the low DMBA exposure, with no impact of a higher exposure. *Gstpi* follows a temporal and concentration dependent pattern of increase with an increase in the high DMBA after 1d, but low DMBA after 4d. These data demonstrate that even low-level exposures activate the ovarian response to xenobiotic exposure, and underscore the importance of the timepoint examined in terms of an ovarian response to an ovotoxic exposure. GSTMU and GSTPI are thus likely involved in ovarian DMBA biotransformation, however, it remains unclear which role (regulation of detoxification or apoptosis) of GSTPI and GSTMU predominates during ovarian DMBA exposure. However, it is clear that these data are in agreement with those previously demonstrated in cultured rat pre-ovulatory follicles, though the DMBA concentrations used in that study were higher than our treatments (Tsai-Turton *et al*., 2007).

EPHX1 is increased in response to ovarian DMBA exposure and bioactivates DMBA to the ovotoxic metabolite DMBA-3,4-diol, 1,2-epoxide (Rajapaksa *et al.*, 2007; Igawa *et al.*, 2009; Nteeba *et al*., 2014). Interestingly, although a trend for an increase in *Ephx1* mRNA at the 75 nM DMBA concentration was observed, the low DMBA had a greater increase in *Ephx1* after 4d of exposure. This could potentially result in increased bioactivation of DMBA to the more ovotoxic metabolite. Although increased EPHX1 protein was not observed in the current study it is possible that basal EPHX1 is depleted by low concentrations of DMBA at a higher rate than high DMBA, and that this potentially results in increased *Ephx1* mRNA as a feedback mechanism, though this has not previously been reported for *Ephx1*. If this is the case, ovaries treated with low DMBA could therefore be exposed to higher amounts of the ovotoxic DMBA metabolite, while lack of any increase in

Ephx1 mRNA in the high DMBA-treated ovaries may indicate less biotransformation of DMBA to the active form above the normal ovarian level due to basal EPHX1 contribution.

Oxidative stress contributes to DMBA-induced follicular apoptosis likely through formation of ROS (Tsai-Turton *et al.*, 2007), and *Sod1* and *Sod2* play essential roles in the detoxification of ROS. *Sod1* was increased by low DMBA after 2d with a trend for an increase after 4d of exposure, and after 4d by the high DMBA. Interestingly, *Sod2* was increased by high DMBA with only a trend for an increase by low DMBA exposure at the same timepoint. These data suggest that ROS are formed following DMBA treatment and the ovary induces an oxidative stress response to combat the harmful oxygen molecules. Previous studies have shown that large pre-antral and antral follicles are particularly sensitive to ROS, in contrast to primordial and small primary follicles which are more resistant, thus an increase in ROS at the low DMBA exposure may partially explain the loss of secondary follicles (Devine *et al.*, 2002; Tsai-Turton *et al.*, 2007). These findings provide additional evidence that DMBA induces production of ROS in the ovary, and that oxidative stress may play a role in DMBA-induced follicle depletion.

Cigarette smoke exposure increases expression of genes involved in the autophagy response in mouse ovaries (Gannon *et al.*, 2012). We observed that, in the cultured rat ovary, compared to control, *Atg7* is decreased by low but not high DMBA exposure. *Becn1* mRNA levels increased after both treatments, again demonstrating temporal pattern of elevation which peaks in the high before the low DMBA. In addition, increases in BECN1 foci were observed at the low DMBA exposure. Autophagy may be activated as a means of follicle depletion and involved in DMBA-induced follicle loss, consistent with data in cigarette-smoke exposed mouse ovaries (Gannon *et al.*, 2012). These results add to the growing number of studies generating evidence for ovarian autophagy playing an active role in follicle depletion.

PI3K signaling is essential for primordial and small primary follicle viability, regulation of follicular recruitment into the growing pool (Yoshida *et al.*, 1997; Parrott and Skinner, 1999; Castrillon *et al.*, 2003) and for regulation of ovarian xenobiotic metabolism gene expression (Bhattacharya and Keating, 2012). The key components of this signaling pathway investigated in this study were the granulosa expressed ligand, *Kitlg*; the oocyte receptor, *cKit*; and the signaling molecule, *Akt1*. It is worth noting that the earliest observed mRNA change in this study was that of *Akt1*. Low DMBA exposure increased mRNA levels of *Kitlg* and *Akt1* while high DMBA exposure also increased Kitlg, earlier than the low treatment, and increased *Akt1* also at an earlier timepoint. Interestingly, no impact of either DMBA exposure on *cKit* was observed. However, cKIT protein was reduced, but the proxy molecule for PI3K activation, $pAKT^{Thr308}$ was increased by both DMBA concentrations, supporting increased PI3K activation. This increase in the PI3K pathway could partially explain why the primordial and small primary follicles were protected from DMBA exposure. PI3K inhibition increases DMBA-induced primordial and small primary follicle loss (Keating *et al.*, 2009), thus our data supports that finding because the induction of the PI3K pathway observed may have prevented primordial and primary follicle loss.

The data herein support that acute low-level exposure to DMBA is a concern for female fertility due to depletion of large primary and secondary follicles, and is consistent with the reduced fecundity experienced by many female smokers (Baird and Wilcox, 1985; Alderete *et al.*, 1995). While large primary were depleted by both DMBA exposures, and secondary follicles lost only during the low exposure, it is worth considering that the numbers within these follicle classes are low, thus small changes can appear significantly different, thus, we consider it premature to assume that differential follicle loss occurred. Undoubtedly however, low concentrations of DMBA depleted large ovarian preantral follicles. Also, genes involved in xenobiotic biotransformation, the oxidative stress response, autophagy and PI3K signaling are activated as part of the ovarian response to DMBA exposure.

Acknowledgments

Conflict of Interest Statement:

The project described was supported by award number R00ES016818 to AFK and R01ES09246 to PBH from the National Institutes of Environmental Health Sciences. The content is solely the responsibility of the authors and does not necessarily represent the official views of the National Institute of Environmental Health Sciences or the National Institutes of Health.

References Cited

Alderete E, Eskenazi B, Sholtz R. Effect of cigarette smoking and coffee drinking on time to conception. Epidemiol. 1995; 6:403–408.

Baird DD, Wilcox AJ. Cigarette smoking associated with delayed conception. JAMA. 1985; 253:2979–2983. [PubMed: 3999259]

Bhattacharya P, Keating AF. Protective role for ovarian glutathione S-transferase isoform pi during 7,12-dimethylbenz[a]anthracene-induced ovotoxicity. Toxicol. Applied Pharmacol. 2012; 260:201–208.

Bhattacharya P, Madden JA, Sen N, Hoyer PB, Keating AF. Glutathione S-transferase class mu regulation of apoptosis signal-regulating kinase 1 protein during VCD-induced ovotoxicity in neonatal rat ovaries. Toxicol. Applied Pharmacol. 2013; 267:49–56.

Bhattacharya P, Sen N, Hoyer PB, Keating AF. Ovarian expressed microsomal epoxide hydrolase: role in detoxification of 4-vinylcyclohexene diepoxide and regulation by phosphatidylinositol-3 kinase signaling. Toxicol. Applied Pharmacol. 2012; 258:118–123.

Borman SM, Christian PJ, Sipes IG, Hoyer PB. Ovotoxicity in female Fischer rats and B6 mice induced by low-concentration exposure to three polycyclic aromatic hydrocarbons: comparison through calculation of an ovotoxic index. Toxicol. Applied Pharmacol. 2000; 167:191–198.

Castrillon DH, Miao L, Kollipara R, Horner JW, DePinho RA. Suppression of ovarian follicle activation in mice by the transcription factor Foxo3a. Science. 2003; 301:215–218. [PubMed: 12855809]

Devine PJ, Sipes IG, Skinner MK, Hoyer PB. Characterization of a Rat in Vitro Ovarian Culture System to Study the Ovarian Toxicant 4-Vinylcyclohexene Diepoxide. Toxicol. Applied Pharmacol. 2002; 184:107–115.

Flaws JA, Doerr JK, Sipes IG, Hoyer PB. Destruction of preantral follicles in adult rats by 4-vinyl-1-cyclohexene diepoxide. Reprod. Toxicol. 1994; 8:509–514. [PubMed: 7881202]

Gannon AM, Stampfli MR, Foster WG. Cigarette smoke exposure elicits increased autophagy and dysregulation of mitochondrial dynamics in murine granulosa cells. Biol Reprod. 2013; 88(3):63. [PubMed: 23325812]

Gannon AM, Stampfli MR, Foster WG. Cigarette smoke exposure leads to follicle loss via an alternative ovarian cell death pathway in a mouse model. Toxicol. Sci. 2012; 125:274–284. [PubMed: 22003194]

Gawriluk TR, Hale AN, Flaws JA, Dillon CP, Green DR, Rucker EB 3rd. Autophagy is a cell survival program for female germ cells in the murine ovary. Reproduction. 2011; 141:759–765. [PubMed: 21464117]

Gelboin HV. Benzo[alpha]pyrene metabolism, activation and carcinogenesis: role and regulation of mixed-function oxidases and related enzymes. Physiolog. Rev. 1980; 60:1107–1166.

Greendale GA, Lee NP, Arriola ER. The menopause. Lancet. 1999; 353:571–580. [PubMed: 10028999]

Henderson CJ, Smith AG, Ure J, Brown K, Bacon EJ, Wolf CR. Increased skin tumorigenesis in mice lacking pi class glutathione S-transferases. PNAS. 1998; 95:5275–5280. [PubMed: 9560266]

Ho YS, Gargano M, Cao J, Bronson RT, Heimler I, Hutz RJ. Reduced fertility in female mice lacking copper-zinc superoxide dismutase. J. Biol. Chem. 1998; 273:7765–7769. [PubMed: 9516486]

Hu X, Christian P, Sipes IG, Hoyer PB. Expression and redistribution of cellular Bad, Bax, and Bcl-X(L) protein is associated with VCD-induced ovotoxicity in rats. Biol. Reprod. 2001; 65:1489–1495. [PubMed: 11673266]

Igawa Y, Keating AF, Rajapaksa KS, Sipes IG, Hoyer PB. Evaluation of ovotoxicity induced by 7, 12-dimethylbenz[a]anthracene and its 3,4-diol metabolite utilizing a rat in vitro ovarian culture system. Toxicol. Applied Pharmacol. 2009; 234:361–369.

Ismail RS, Okawara Y, Fryer JN, Vanderhyden BC. Hormonal regulation of the ligand for c-kit in the rat ovary and its effects on spontaneous oocyte meiotic maturation. Mol. Reprod. Dev. 1996; 43:458–469. [PubMed: 9052937]

Jick H, Porter J. Relation between smoking and age of natural menopause. Report from the Boston Collaborative Drug Surveillance Program, Boston University Medical Center. Lancet. 1977; 1:1354–1355. [PubMed: 69066]

John GB, Gallardo TD, Shirley LJ, Castrillon DH. Foxo3 is a PI3K-dependent molecular switch controlling the initiation of oocyte growth. Dev. Biol. 2008; 321:197–204. [PubMed: 18601916]

Keating AF, Mark CJ, Sen N, Sipes IG, Hoyer PB. Effect of phosphatidylinositol-3 kinase inhibition on ovotoxicity caused by 4-vinylcyclohexene diepoxide and 7, 12-dimethylbenz[a]anthracene in neonatal rat ovaries. Toxicol. Applied Pharmacol. 2009; 241:127–134.

Keating AF, Rajapaksa KS, Sipes IG, Hoyer PB. Effect of CYP2E1 gene deletion in mice on expression of microsomal epoxide hydrolase in response to VCD exposure. Toxicol. Sci. 2008; 105:351–359. [PubMed: 18622027]

Keating AF, Sen N, Sipes IG, Hoyer PB. Dual protective role for glutathione S-transferase class pi against VCD-induced ovotoxicity in the rat ovary. Toxicol. Applied Pharmacol. 2010; 247:71–75.

Kim J, Dalton VM, Eggerton KP, Scott SV, Klionsky DJ. Apg7p/Cvt2p is required for the cytoplasm-to-vacuole targeting, macroautophagy, and peroxisome degradation pathways. Mol. Biol. Cell. 1999; 10:1337–1351. [PubMed: 10233148]

Kim SK, Woodcroft KJ, Kim SG, Novak RF. Insulin and glucagon signaling in regulation of microsomal epoxide hydrolase expression in primary cultured rat hepatocytes. Drug Metab. Disp. 2003; 31:1260–1268.

Levine B, Klionsky DJ. Development by self-digestion: molecular mechanisms and biological functions of autophagy. Devel. Cell. 2004; 6:463–477. [PubMed: 15068787]

Liang XH, Jackson S, Seaman M, Brown K, Kempkes B, Hibshoosh H, Levine B. Induction of autophagy and inhibition of tumorigenesis by beclin 1. Nature. 1999; 402:672–676. [PubMed: 10604474]

Liu K, Rajareddy S, Liu L, Jagarlamudi K, Boman K, Selstam G, Reddy P. Control of mammalian oocyte growth and early follicular development by the oocyte PI3 kinase pathway: new roles for an old timer. Dev. Biol. 2006; 299:1–11. [PubMed: 16970938]

Livak KJ, Schmittgen TD. Analysis of relative gene expression data using real-time quantitative PCR and the 2(-Delta Delta C(T)) Method. Methods. 2001; 25:402–408. [PubMed: 11846609]

Mattison DR. Difference in sensitivity of rat and mouse primordial oocytes to destruction by polycyclic aromatic hydrocarbons. Chem. Biol. Interact. 1979; 28:133–137. [PubMed: 115601]

Mattison DR, Schulman JD. How xenobiotic chemicals can destroy oocytes. Contemp. Obstet. Gynecol. 1980; 15:157.

Mattison DR, Thorgeirsson SS. Ovarian aryl hydrocarbon hydroxylase activity and primordial oocyte toxicity of polycyclic aromatic hydrocarbons in mice. Cancer Res. 1979; 39:3471–3475. [PubMed: 113091]

Matzuk MM, Dionne L, Guo Q, Kumar TR, Lebovitz RM. Ovarian function in superoxide dismutase 1 and 2 knockout mice. Endocrinol. 1998; 139:4008–4011.

Miyata M, Kudo G, Lee YH, Yang TJ, Gelboin HV, Fernandez-Salguero P, Kimura S, Gonzalez FJ. Targeted disruption of the microsomal epoxide hydrolase gene. Microsomal epoxide hydrolase is required for the carcinogenic activity of 7,12-dimethylbenz[a]anthracene. J. Biol. Chem. 1999; 274:23963–23968. [PubMed: 10446164]

Morita Y, Tilly JL. Oocyte apoptosis: like sand through an hourglass. Dev. Biol. 1999; 213:1–17. [PubMed: 10452843]

Nteeba J, Ganesan S, Keating AF. Impact of obesity on ovotoxicity induced by 7,12-dimethylbenz[a]anthracene in mice. Biol. Reprod. 2014 In Press.

Parrott JA, Skinner MK. Kit-ligand/stem cell factor induces primordial follicle development and initiates folliculogenesis. Endocrinol. 1999; 140:4262–4271.

Pfaffl MW. A new mathematical model for relative quantification in real-time RT-PCR. Nucleic Acids Res. 2001; 29:e45. [PubMed: 11328886]

Rajapaksa KS, Sipes IG, Hoyer PB. involvement of microsomal epoxide hydrolase enzyme in ovotoxicity caused by 7,12-dimethylbenz[a]anthracene. Toxicol. Sci. 2007; 96:327–334. [PubMed: 17204581]

Reddy CC, Burgess JR, Gong ZZ, Massaro EJ, Tu CP. Purification and characterization of the individual glutathione S-transferases from sheep liver. Arch. Biochem. Biophys. 1983; 224:87–101. [PubMed: 6870266]

Reddy P, Shen L, Ren C, Boman K, Lundin E, Ottander U, Lindgren P, Liu YX, Sun QY, Liu K. Activation of Akt (PKB) and suppression of FKHRL1 in mouse and rat oocytes by stem cell factor during follicular activation and development. Dev. Biol. 2005; 281:160–170. [PubMed: 15893970]

Smith BJ, Mattison DR, Sipes IG. The role of epoxidation in 4-vinylcyclohexene-induced ovarian toxicity. Toxicol. Applied Pharmacol. 1990; 105:372–381.

Tsai-Turton M, Nakamura BN, Luderer U. Induction of apoptosis by 9,10-dimethyl-1,2-benzanthracene in cultured preovulatory rat follicles is preceded by a rise in reactive oxygen species and is prevented by glutathione. Biol. Reprod. 2007; 77:442–451. [PubMed: 17554082]

Yoshida H, Takakura N, Kataoka H, Kunisada T, Okamura H, Nishikawa SI. Stepwise requirement of c-kit tyrosine kinase in mouse ovarian follicle development. Dev. Biol. 1997; 184:122–137. [PubMed: 9142989]

Highlights

- Acute DMBA exposures induce large primary and/or secondary follicle loss.
- Acute DMBA exposure did not impact primordial and small primary follicle number.
- Altered ovarian gene expression was observed due to DMBA exposure.

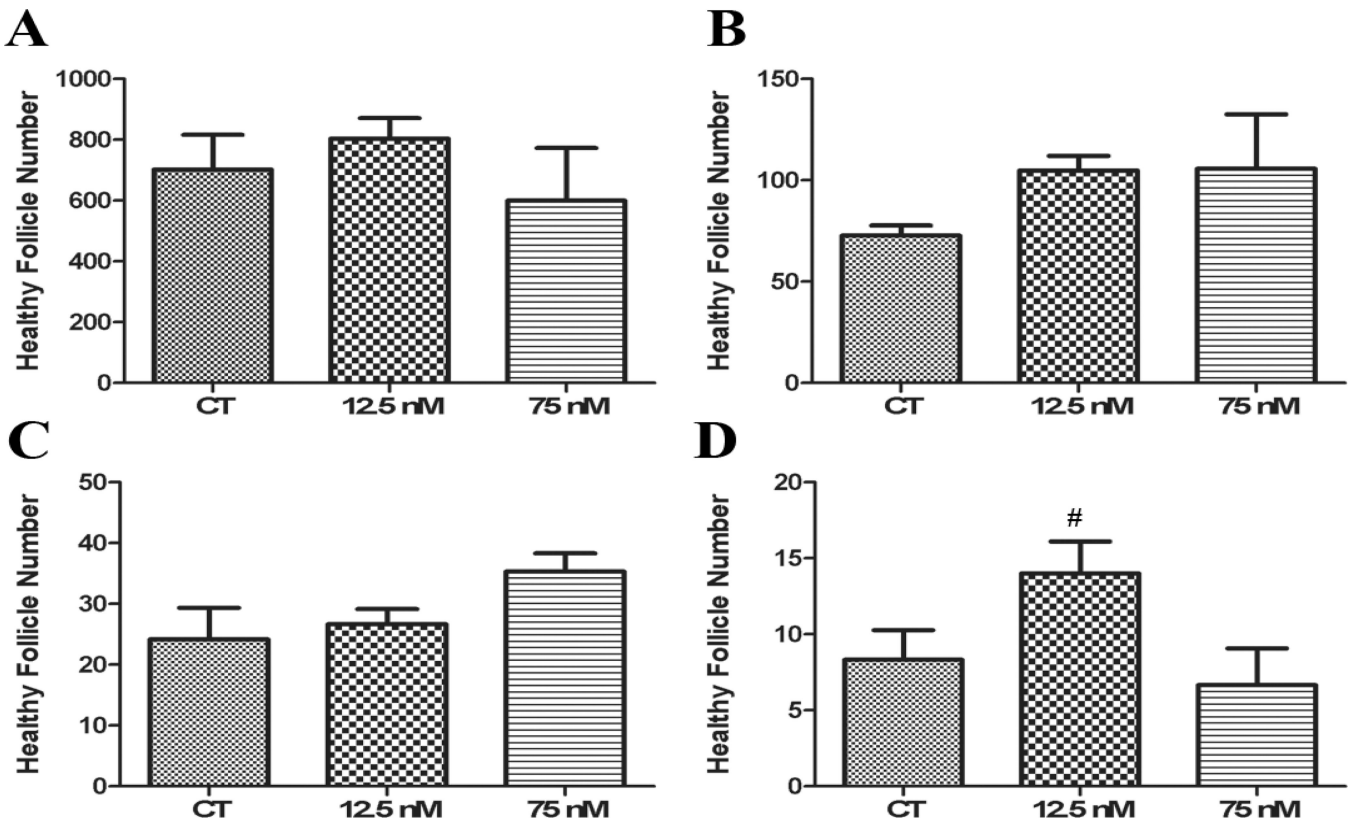

Figure 1. Impact of single DMBA exposure on follicle morphology and number

PND4 rat ovaries were cultured for 4 d in control media and thereafter exposed once to 1% DMSO (vehicle control) or 12.5 nM DMBA or 75 nM DMBA. Following four additional days of culture, follicles were classified and counted: (A) Primordial Follicles; (B) Small Primary Follicles; (C) Large Primary Follicles; (D) Secondary Follicles. Values represent mean ± SE total follicles counted/ovary, n=5. $^{\#} = P < 0.1$.

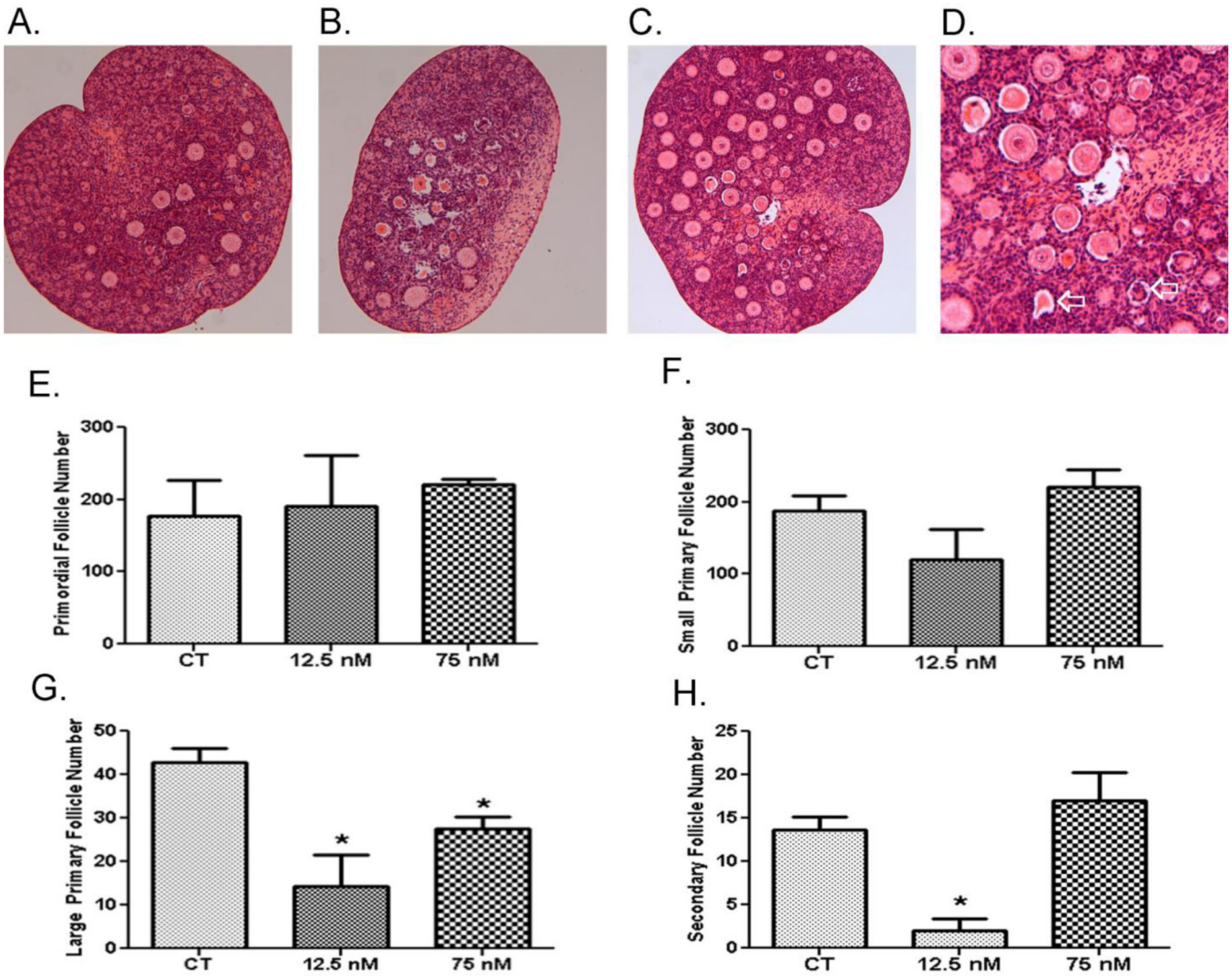

Figure 2. Effect of single DMBA exposure on follicle morphology and number

PND4 rat ovaries were cultured for 4 d in control media and thereafter exposed once to (A) 1% DMSO (vehicle control) or (B) 12.5 nM DMBA or (C) 75 nM DMBA. D depicts DMBA-induced shrunken oocytes indicated by the open arrow. Following eight additional days of culture, follicles were classified and counted: (E) Primordial Follicles; (F) Small Primary Follicles; (G) Large Primary Follicles; (H) Secondary Follicles. Values (E–H) represent mean ± SE total follicles counted/ovary, n=5; * = different from control in each follicle type, $P < 0.05$.

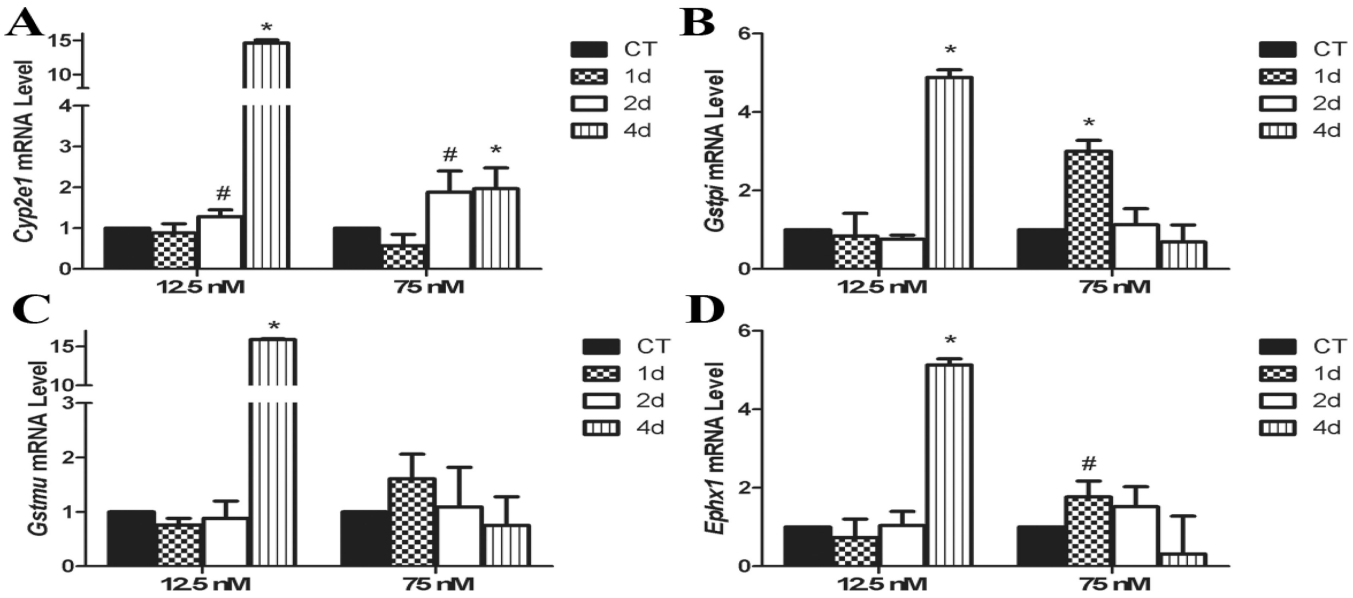

Figure 3. Effect of DMBA on ovarian expression of chemical biotransformation genes

PND4 rat ovaries were cultured for 4 d in control media and thereafter exposed to a single 1% DMSO (vehicle control) or DMBA (12.5 nM or 75 nM). Following 1, 2 or 4 additional days of culture, mRNA was isolated and (A) *Cyp2e1*, (B) *Gstp*, (C) *Gstm*, and (D) *Ephx1* levels evaluated by quantitative RT-PCR. Values represent fold-change ± SEM relative to a control value of 1, normalized to *Gapdh*. * = different from control, $P < 0.05$; # = $P < 0.1$.

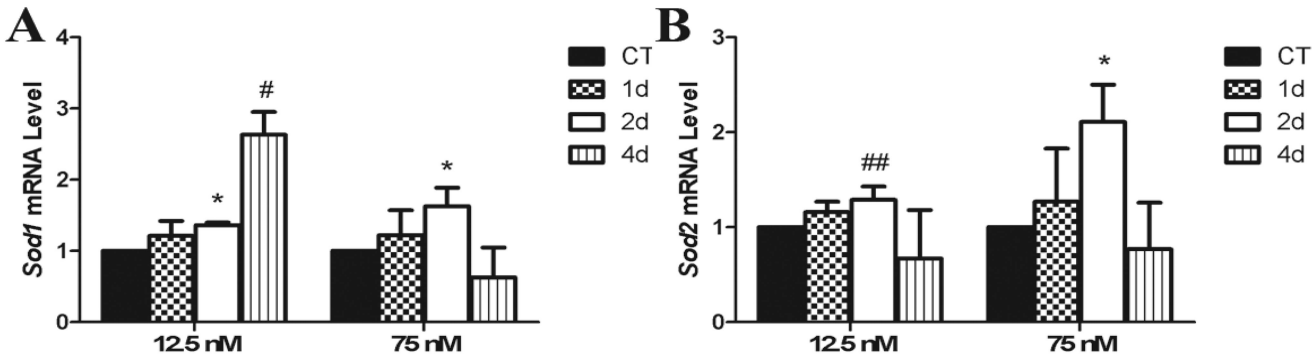

Figure 4. Effect of DMBA on ovarian expression of reactive oxygen species metabolism genes

PND4 rat ovaries were cultured for 4 d in control media and thereafter exposed to a single 1% DMSO (vehicle control) or DMBA (12.5 nM or 75 nM). Following 1, 2 or 4 additional days of culture, mRNA was isolated and (A) *Sod1* or (B) *Sod2* levels evaluated by quantitative RT-PCR. Values represent fold-change ± SEM relative to a control value of 1, normalized to *Gapdh*. * = different from control, $P < 0.05$; # = $P < 0.1$. ## = $P = 0.1$.

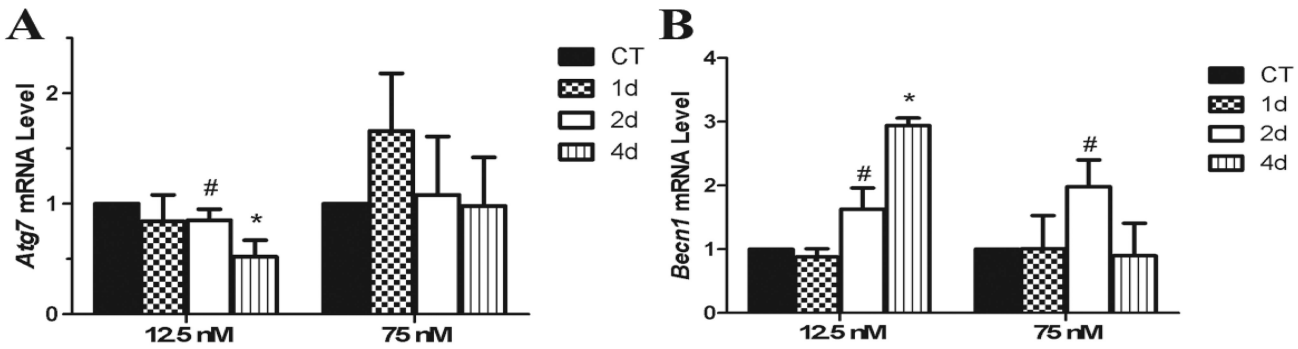

Figure 5. Effect of DMBA on ovarian expression of autophagy genes

PND4 rat ovaries were cultured for 4 d in control media and thereafter exposed to a single 1% DMSO (vehicle control) or DMBA (12.5 nM or 75 nM). Following 1, 2 or 4 additional days of culture, mRNA was isolated and (A) *Atg7* or (B) *Becn1* levels evaluated by quantitative RT-PCR. Values represent fold-change ± SEM relative to a control value of 1, normalized to *Gapdh*. * = different from control, $P < 0.05$; $^{\#} = P < 0.1$.

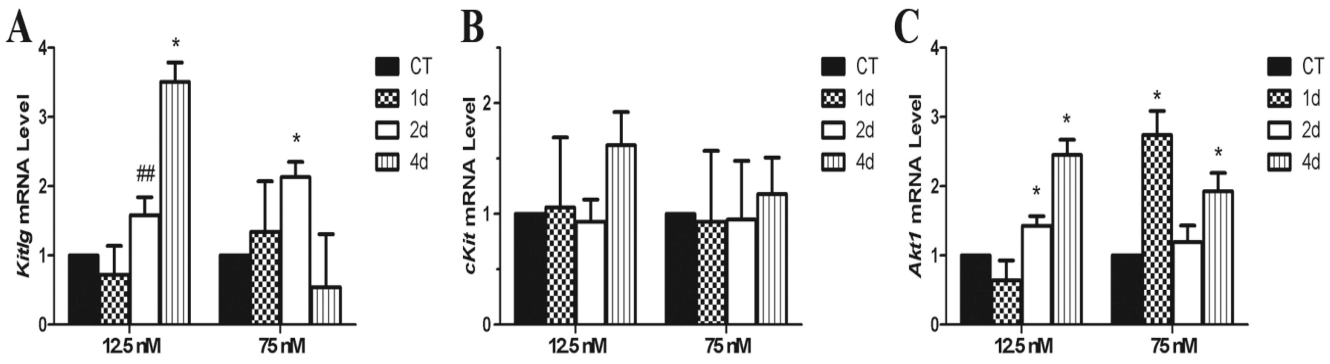

Figure 6. Effect of DMBA on ovarian expression of autophagy genes

PND4 rat ovaries were cultured for 4 d in control media and thereafter exposed to a single 1% DMSO (vehicle control) or DMBA (12.5 nM or 75 nM). Following 1, 2 or 4 additional days of culture, mRNA was isolated and (A) *Kitlg* or (B) *cKit* or (C) *Akt1* levels evaluated by quantitative RT-PCR. Values represent fold-change ± SEM relative to a control value of 1, normalized to *Gapdh*. * = different from control, $P < 0.05$; # = $P < 0.1$.

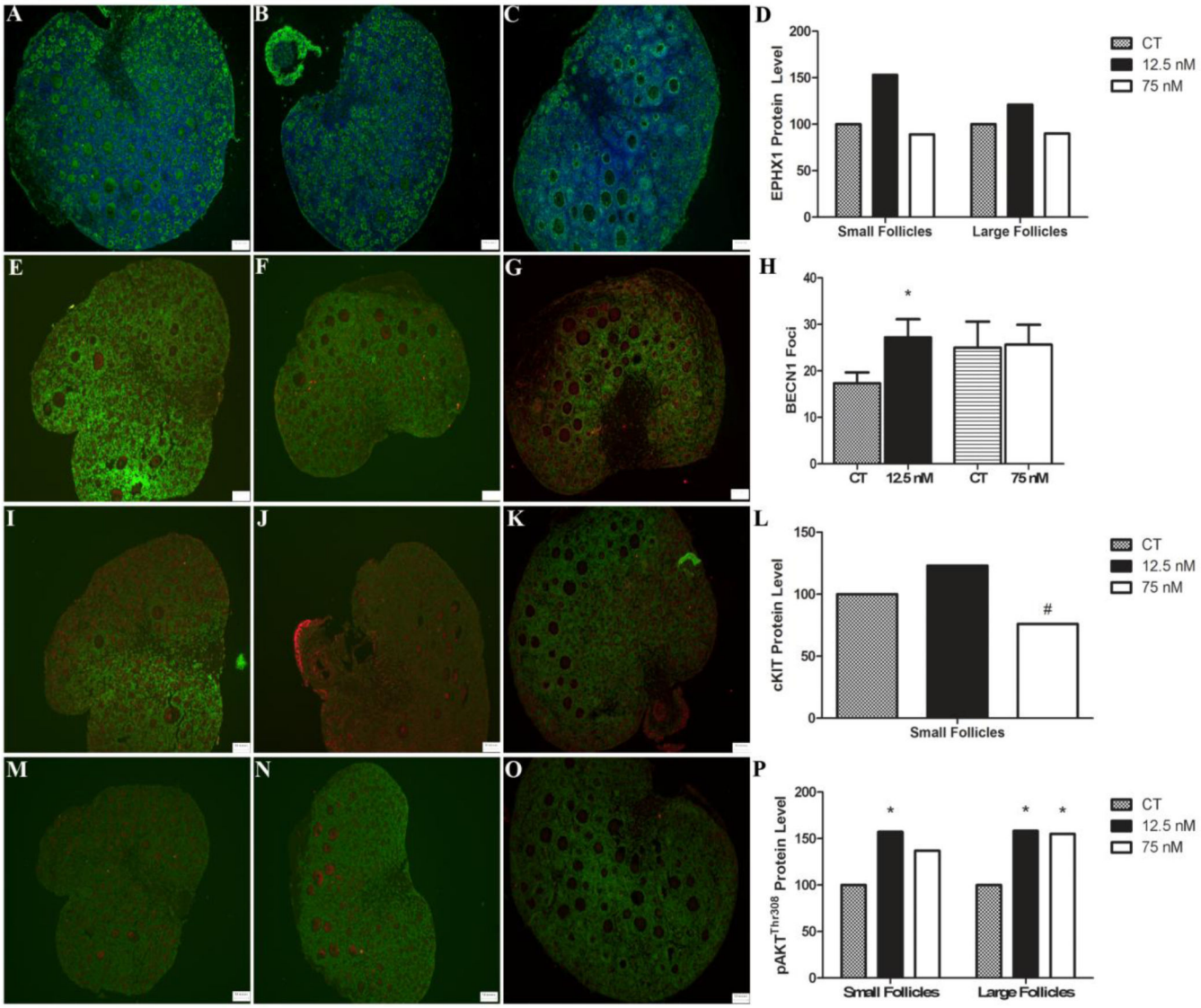

Figure 7. Localization and effect of DMBA on ovarian EPHX1, BECN1, cKIT or pAKT^{Thr308} protein

PND4 rat ovaries were cultured for 4 d in control media and thereafter exposed to a single (A) 1% DMSO (vehicle control) (B) 12.5 nM DMBA or (C) 75 nM DMBA. Following four additional days of culture, ovaries were fixed in formalin, and immunofluorescence staining was performed using a primary antibody directed against (A–C) EPHX1, (E–G) BECN1, (I–K) cKIT or pAKT^{Thr308}. EPHX1 is represented in green and the Hoechst nuclear stain is in blue. BECN1, cKIT and pAKT^{Thr308} are represented in red and the Hoechst nuclear stain is in green. Quantification of (D) EPHX1, (H) BECN1, (L) cKIT or (P) pAKT^{Thr308} was performed and * = different from control, $P < 0.05$; $^{\#} = P < 0.1$.

Table 1

Primers used in real-time PCR

Gene	Forward (5'-3')	Reverse (3'-5')
Ephx1	GGCTCAAAGCCATCAGGCA	AAAGTGGTGTCTTCTGGAGG
GSTp	GGCATCTGAAGCCTTTTGAG	GCTCTCTGCCTATGTGGCTC
GSTm	TTCAAGCTGGGCCTGGAC	CAGAGCAATGCCATCCTG
Cyp2e1	CGTGTGTGTGTTGGAGAAGG	TACTGCCAAAGCCAACTGTG
Sod1	GGAGAGCATTCCATCATTGG	CAATCACACCACAAGCCAAG
Sod2	GCCTTTGTGAATTTGCCTTT	CTGACCACAGCCTTTTTGGT
Atg7	CTTCCTGGCCAAGGTGTTTA	GTTGCTCAGACGGTCTCCTC
Becn1	TAATGTGGGGAAGGGACAAG	AAATCCTTCCACATCTCAAACA
Kitlg	GGCCTACAATGGACAGCAAT	TCAACTGCCCTTGTAAGACTT
cKit	CTTTTGCGCAAGCTTTTGT	ATCCCCCGCTCCAAAGTAT
Akt1	ACCTCTGAGACCGACCGACACCAG	ACTTTCCCCAGTTCTCCT
Gapdh	GGATGGAATTGTGAGGGAGA	GTGGACCTCATGGCCTACAT